



Contents lists available at ScienceDirect

Chinese Chemical Letters

journal homepage: [www.elsevier.com/locate/cclet](http://www.elsevier.com/locate/cclet)

Communication

## A photoelectrochemical cell for pollutant degradation and simultaneous H<sub>2</sub> generation

Jin Han<sup>a</sup>, Yaru Bian<sup>b</sup>, Xiuzhen Zheng<sup>a</sup>, Xiaoming Sun<sup>b</sup>, Liwu Zhang<sup>a,\*</sup><sup>a</sup> Department of Environmental Science and Engineering, Fudan University, Shanghai 200433, China<sup>b</sup> College of Science, Beijing University of Chemistry Technology, Beijing 100029, China

## ARTICLE INFO

## Article history:

Received 2 May 2017

Received in revised form 12 August 2017

Accepted 15 August 2017

Available online xxx

## Keywords:

Solar energy

Hydrogen

Azo dye

PEC

BiVO<sub>4</sub>

## ABSTRACT

A visible-light driven photoelectrochemical (PEC) cell comprised of nanostructured BiVO<sub>4</sub> photoanode and Pt cathode was established for organic compounds degradation with simultaneous H<sub>2</sub> generation. BiVO<sub>4</sub> electrode film fabricated by a simple drip-coating method showed a porous nanostructure and an intense absorption in visible light range. The PEC process possesses a rate of about 0.3207 h<sup>-1</sup> for MO degradation, which is 8 times and 64 times faster than electrocatalytic (EC) and photocatalytic (PC) process, respectively. A simultaneous H<sub>2</sub> generation via the PEC process was also observed and a rate of 34.44 μmol h<sup>-1</sup> cm<sup>-2</sup> for H<sub>2</sub> generation was measured, which is 3 folds more efficient than the EC process. The nanostructured BiVO<sub>4</sub> photoanode shows outstanding PEC photocurrent density and recycle performance. The proposed PEC system would be a promising strategy for wastewater treatment and energy recovery with an outstanding stability and recyclability performance.

© 2017 Chinese Chemical Society and Institute of Materia Medica, Chinese Academy of Medical Sciences. Published by Elsevier B.V. All rights reserved.

The combustion of the fossil fuel not only leads to the growing worldwide energy crisis, but also causes serious environmental pollution problem, such as the acid deposition, haze and the formation of PM<sub>2.5</sub> [1–4]. Consequently, researches on alternative and clean energy resources have become an urgent challenge for scientists all over the world. There are many possible alternative energy resources could be used as the new energy candidates, such as the solar, wind, geothermal and hydrogen [5]. As a renewable, green, safe and viable energy resource, hydrogen (H<sub>2</sub>), which owns a high gravimetric energy density, has been widely investigated as the next generation energy carrier during the past few decades [6–11].

Till now, many technologies have been developed to produce H<sub>2</sub> [5,12–17]. Water splitting by PEC process has been studied as an environmental friendly and potential route for the transformation from the inexhaustible solar energy to the directly used and green H<sub>2</sub> energy [5,12,18–24]. However, in a typical PEC water splitting process, the half reaction on the photoanode is the O<sub>2</sub> evolution reaction, whose product O<sub>2</sub> is not of significant value. It is more energy efficient if we can replace the O<sub>2</sub> evolution reaction with some more useful oxidation reaction. We thus propose that the wastewater treatment could be integrated to the PEC water

splitting, which may make the PEC water splitting economically feasible [5,8,9,25–28]. The PEC wastewater treatment has been reported by many researchers [8,29]. In this process, the organics dye in wastewater is oxidized at the anode, while the H<sub>2</sub> is generated at the cathode. Thus, H<sub>2</sub> generation can be well integrated into the PEC of wastewater treatment simultaneously.

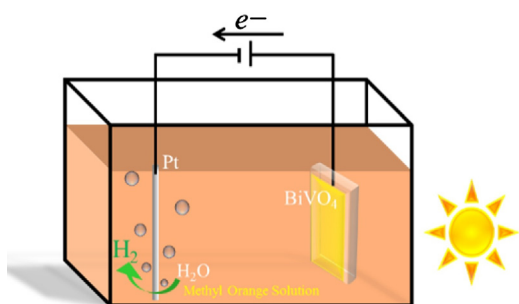
As an n-type semiconductor, bismuth vanadate (BiVO<sub>4</sub>), which owns a narrow band gap (2.4 eV) and a broad response in visible light range, has been considered as one of the most promising photoanode candidates for water splitting [18,19,30–32]. Besides, many references reported it has a high oxidation ability and excellent stability for oxidation degradation [33,34]. Herein, we use a nanostructured BiVO<sub>4</sub> film as the photoanode for the oxidation of azo dye with a simultaneously H<sub>2</sub> production on the cathode. As shown in Scheme 1, a two electrodes configuration was employed with a Pt wire as the counter electrode, while BiVO<sub>4</sub> as the working electrode, and electrolyte is the solution of azo dye in Na<sub>2</sub>SO<sub>4</sub>. During the PEC process, the oxidation of azo dye takes place on the anode, while water is reduced on the cathode to produce H<sub>2</sub>.

All chemical reagents are analytical grade and used without any further purification. Deionized water was used throughout the whole experiment. FTO glasses were sonicated by immersing in the acetone, ethanol and DI water in sequence to remove the impurities that existed in the surface of the FTO glasses.

\* Corresponding author.

E-mail address: [zhanglw@fudan.edu.cn](mailto:zhanglw@fudan.edu.cn) (L. Zhang).<http://dx.doi.org/10.1016/j.cclet.2017.08.031>

1001-8417/© 2017 Chinese Chemical Society and Institute of Materia Medica, Chinese Academy of Medical Sciences. Published by Elsevier B.V. All rights reserved.



**Scheme 1.** Experimental device for methyl orange degradation with simultaneous  $\text{H}_2$  generation via PEC route by nanostructured  $\text{BiVO}_4$ .

The  $\text{BiVO}_4/\text{FTO}$  was synthesized by a drop-coating method of the  $\text{BiVO}_4$  precursor solution onto the conducting plane of the FTO. In a typical procedure, 0.5 mmol of  $\text{Bi}(\text{NO}_3)_3 \cdot 5\text{H}_2\text{O}$ , 0.5 mmol  $\text{NH}_4\text{VO}_3$  were dissolved in the mixture of 5 mL nitric acid and 5 mL DI water. After the solute was dissolved, 5 mL of ethanol was added to dilute the mixture. Then the  $\text{BiVO}_4$  precursor (40  $\mu\text{L}$ ) was dripped to the surface of FTO. After dried at 60 °C in an oven, the catalysts were calcined at 500 °C for 3 h with a ramping rate of 2 °C/min.

The microstructure of as-prepared electrode was characterized with scanning electron microscopy (SEM, Philips XL30FEG, Netherlands). The crystal structure of the as-prepared electrode was measured using X-ray diffraction (XRD) patterns by a Druker with  $\text{Cu K}\alpha$  radiation ranging from 10° to 70°. UV–vis spectrum of the as-prepared electrode was performed using a UV–vis spectrophotometer (SHIMADZU UV-2600) with an integrating sphere attachment. The change in the total organic carbon (TOC) of MO solution after degradation was tested using TOC analyzer (TOC 2500, Shimadzu, Japan). X-ray photoelectron spectroscopy (XPS) was performed on a Perkin-Elmer PHI-5000C ESCA system equipped with a dual X-ray source, using an Mg  $\text{K}\alpha$  radiation source and a hemispherical energy analyzer. Linear Sweep Voltammetry (LSV) measurements were carried out by an electrochemical station (CHI 660E, Shanghai Chenhua Co., Ltd. China).

During the photoelectrochemical tests, a standard three electrodes configuration were employed, the synthesized  $\text{BiVO}_4$  film is used as the working electrode, Pt wire as the counter electrode and  $\text{Ag}/\text{AgCl}$  as the reference electrode. The potential conversion from vs.  $\text{Ag}/\text{AgCl}$  to vs. reversible hydrogen electrode (RHE) was calculated using Eq. (1):

$$E(\text{vs. RHE}) = E(\text{vs. Ag/AgCl}) + 0.199 \text{ V} + 0.0591 \text{ pH} \quad (1)$$

The PEC degradation of organic contaminant and the amounts of  $\text{H}_2$  were performed in a PEC reactor in a two-electrode system at 3.5 V under an air mass (AM) 1.5 G radiation in a 200 mL reactor with 120 mL solution filled in. As the protective gas, Ar was

bubbled into the reactor cell. The size of the synthesized mesoporous film electrode is  $1 \times 1 \text{ cm}^2$ . 300 W Xe lamp was used as the artificial solar light source and illuminate from the back side of the film. The working electrode was illuminated from the light source through a quartz window of the reactor cell. The bias voltage applied to the film electrode was supplied by the electrochemical a potentiostat. In this system, methyl orange (MO, 10 ppm) was used as an azo dye during the PEC process. And the  $\text{Na}_2\text{SO}_4$  (0.5 mol/L) was used as the supporting electrolyte. The adsorption spectra and contents of the MO in the solution were measured by UV–vis spectrophotometer (SHIMADZU UV-2600). The degradation ration of MO was defined in Eq. (2):

$$C_t/C_0 \times 100\% \quad (2)$$

where  $C_0$  is the initial concentration of MO in the solution;  $C_t$  denotes the concentration of MO at the different moment. HPLC was performed by an Agilent 1100 Series. Samples were separated on a Zorbax SB  $\text{C}_{18}$  (4.6 mm  $\times$  150 mm, 5  $\mu\text{m}$ ) reverse phase column at 50 °C. The mobile phase consisting of methanol/water = 50:50 (V/V) was set at a flow rate of 0.8 mL/min. The concentration of  $\text{H}_2$  was analyzed by gas chromatography (SHIMADZU, GC-2014) using a thermal conductivity detector (TCD). The theoretical evolution rate of  $\text{H}_2$  is calculated according to the following equation (Eq. (3)):

$$v = I \times t / (Z \times F \times A \times 3600) \quad (3)$$

Where,  $v$  indicates the evolution rate of  $\text{H}_2$  ( $\text{mol cm}^{-2} \text{ h}^{-1}$ );  $I$  indicates the average current (A);  $t$  indicates the time (s);  $Z$  indicates the transferred electron number (1);  $F$  is the Faraday's constant (96500 C/mol);  $A$  is the area of the  $\text{BiVO}_4$  film ( $\text{cm}^2$ ).

The equation for the calculation of Faradaic efficiency is described in Eq. (4):

$$\text{Faradaic efficiency (\%)} = m \times n \times F / (I \times t) \quad (4)$$

Where,  $m$  is the experimental value of  $\text{H}_2$  (mol);  $n$  is the reacted electron number (1);  $F$  is the Faraday's constant (96500 C/mol);  $I$  is the average current (A);  $t$  is the time (s).

The microstructure of the as-prepared  $\text{BiVO}_4$  film is investigated by SEM in Fig. 1a. The film of  $\text{BiVO}_4$  is composed of spherical nanoparticles with diameter of about 500 nm. And the sphere consisted of nanoparticles, with diameter of about 9 nm (Fig. 1b). A  $\text{BiVO}_4$  nanofilm can be successfully synthesized by this simple drip-coating method, the nanofilm shows porous structure, ultrathin thickness and high surface area, which are beneficial for the photoelectrocatalytic oxidation reaction. The XRD experiment is carried out to determine the chemical composition and crystal structure of the photoelectrode, and the obtained XRD spectra of  $\text{BiVO}_4$  and naked FTO are shown in Fig. 1c. It is clear that the diffraction patterns of the synthesized  $\text{BiVO}_4$  is highly consistent with the characteristic reflections of the monoclinic scheelite structure (JCPDS NO. 14-0688), and the sharp peaks of

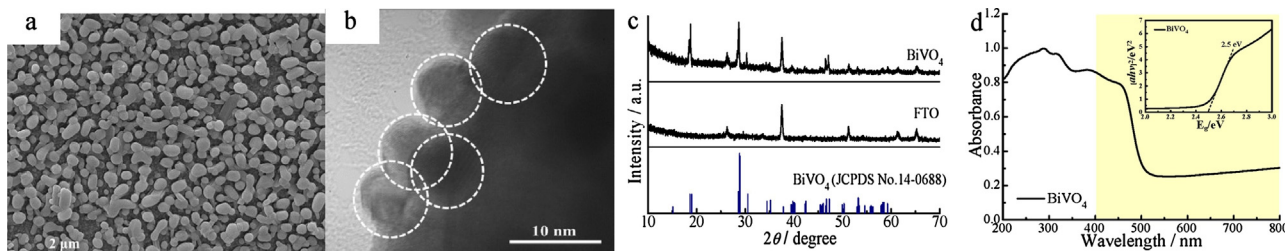


**Fig. 1.** (a) SEM images (b) HRTEM image of nanostructured  $\text{BiVO}_4$  film; (c) XRD patterns of  $\text{BiVO}_4$  and naked FTO; (d) UV–vis absorption spectrum and the Tauc plot of  $\text{BiVO}_4$  (insert).

BiVO<sub>4</sub> film sample indicate it has a good crystallinity. The thickness of the as-prepared BiVO<sub>4</sub> film is thin, as a result, the diffraction peaks of FTO substrate are also observed.

UV-vis diffraction reflection spectroscopy (UV-vis DRS) is conducted to investigate the optical property of the synthesized BiVO<sub>4</sub> film. As shown in Fig. 1d, three broad absorption bands of the synthesized BiVO<sub>4</sub> film are observed at wavelengths of 200–350 nm, 350–420 nm, and 420–500 nm, respectively. Besides, there is a strong absorption in the visible light region ( $\lambda > 420$  nm) for the synthesized BiVO<sub>4</sub> film. And, the band gap of the BiVO<sub>4</sub> film calculated from the Tauc plot is 2.5 eV (Fig. 1d inset), which is in consistence with the reported band gap of BiVO<sub>4</sub> [18]. The BiVO<sub>4</sub> film with an intense absorption from the UV to visible light range could be favor for the efficient utilization of the solar light.

The PEC performances are evaluated both in dark and under AM 1.5 G simulated solar light illumination (100 mW/cm<sup>2</sup>) in the MO solution. Fig. S1a in Supporting information displays the photocurrent density–bias (*J*-*V*) curves of BiVO<sub>4</sub> electrode film in dark and under irradiation by using a three-electrode configuration. It is clearly that the current density is negligible in the dark condition. The detected current increased remarkably when light is turned-on. The nanostructured BiVO<sub>4</sub> electrode film produced an anodic photocurrent demonstrating the n-type nature of BiVO<sub>4</sub> [35]. The transient photocurrent performance is performed to preliminary estimate the charge carrier recombination properties on the interface of the semiconductor. As shown in Fig. S1b, the photocurrent value presents fast and uniform results, alternatively increasing to maximum value and decreased to zero corresponding to the light switched on and off. Besides, the phenomenon of the photoresponse is reversible. It is known that the generated transient anodic photocurrent wave, when the light is turn-on, represents the accumulation of holes at the electrode–electrolyte interface. At the same time, the generated transient cathodic photocurrent wave, when the chopped light is turn-off, represents the recombination of electrons from the conduction band with the accumulated holes. The obtained nanostructured BiVO<sub>4</sub> displays an outstanding photocurrent density compared with the published researches [36,37].

The catalytic activities of the typical azo dye samples are investigated using the degradation of MO at room temperature. The PEC (at a bias potential of 3.5 V with irradiation), EC (electrocatalytic process at a bias potential of 3.5 V, without irradiation), and PC (photocatalytic, without a bias potential) in neutral aqueous solutions are performed under the given conditions. The UV–vis absorption spectra of MO solution are conducted under wavelengths from 200–800 nm during the PEC, EC and PC operations (Fig. 2a and Fig. S2a–b in Supporting information). The MO solution was stirred for 30 min to reach the adsorption equilibrium. The changes of MO concentration *versus* the reaction time over BiVO<sub>4</sub> film during the PEC, EC and PC process were shown in Fig. 2a and Fig. S2a–b in Supporting information, respectively. The major characteristic peak of MO (around 464 nm)

diminishes gradually under the PEC and EC process. However, the PC process test shows that MO is stable under visible light irradiation, indicating that the photolysis of MO is negligible during the whole catalytic period. Meanwhile, the color of the suspension changed gradually during the PEC and EC process, suggesting that the chromophoric structure of MO was decomposed. Additionally, new absorbance peaks that appeared ranging from 210–250 nm indicated the formation of small molecular intermediate products in Fig. 2a. Hence, the activity order of MO degradation is follows the tendency of PEC > EC > PC. The relative concentration ( $C_t/C_0$ ,  $C_t$  and  $C_0$  stand for the remnant and initial concentrations of MO, respectively) as a function of time is shown in Fig. 2b. As shown in Fig. 2b, the BiVO<sub>4</sub> film exhibits the highest catalytic activity via PEC process, which significantly outperformed the same film under the EC and PC process. To further investigate the degradation kinetics, the *pseudo*-first-order kinetic model ( $\ln(C_t/C_0) = -kt$ ,  $k$  is the kinetic constant,  $t$  is the reaction time) is applied to fit the degradation data and the fitting results are shown in Table S1 in Supporting information. As seen in Fig. S2c and Table S1, for the degradation rate of MO, the PEC process obtains the highest rate constant of about 0.3207 h<sup>-1</sup>, which is higher than that of EC (about 0.0421 h<sup>-1</sup>) or PC (about 0.005 h<sup>-1</sup>). The results indicate that the degradation efficiency of MO can be significantly improved under the combination of the photocatalytic process and the electrocatalytic process, which could effectively facilitate the separation of photogenerated electron-hole pairs.

HPLC chromatograms of the MO solution at initial, and after different catalytic route for 6 h are recorded in Fig. 2c. It is remarkably to note that a much lower intensity of MO is presented by PEC route than that of EC or PC route. Besides, the retention time of MO moves forward, indicating the existence of obtained small molecule intermediate from MO during the PEC process. The HPLC results further confirm that the BiVO<sub>4</sub> electrode film exhibits much more excellent degradation performance of MO degradation by PEC process as compared with EC or PC process. Despite its effectiveness in MO decoloration, the catalytic degradation on the BiVO<sub>4</sub> film may not lead to the mineralization. The mineralization depends on whether the refractory intermediate compounds are more difficult to degrade relative to the original substrate. Therefore, TOC measurements are conducted under different catalytic degradation process. As shown in Fig. S2d, 66% of the TOC is removed after discoloration of MO for 6 h with degradation by PEC process. However, with PC process the mineralization of MO took place at a much lower rate and TOC was reduced nearly 5%. Obviously, the rate of the decoloration was much faster than that of mineralization.

The H<sub>2</sub> evolution is also studied at the same time with the MO degradation during the PEC and EC process. Fig. 2d shows the H<sub>2</sub> amount evolved theoretically (calculated from the photocurrent) vs. evolved experimentally by PEC or EC process, and the current density during these two processes are provided as well. In addition, the current densities, theoretical evolution rates of H<sub>2</sub>,

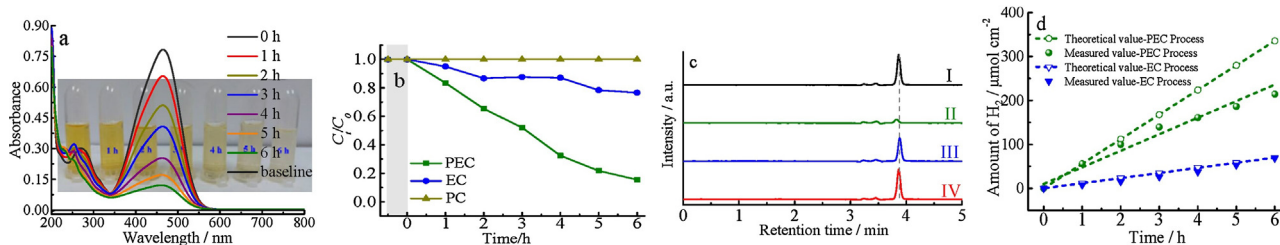


**Fig. 2.** (a) The temporal evolution of UV-vis adsorption spectra and the corresponding optical images of MO solutions at different irradiation time by PEC degradation using the as-prepared BiVO<sub>4</sub> electrode film during visible light irradiation; (b) comparison of degradation performance by PEC, EC and PC process; (c) HPLC chromatograms of the initial MO solution (I) and after 6 h degradation over PEC (II), EC (III) and PC (IV) routes; (d) Amount of hydrogen at an applied potential of 3.5 V in two-electrode system for 6 h.

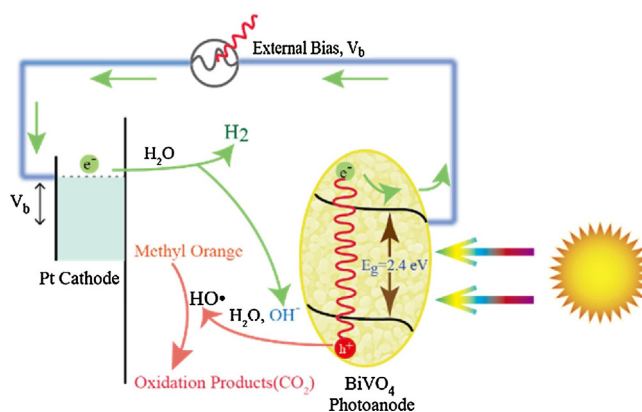
experimental evolution rates of H<sub>2</sub> and the Faradaic efficiencies of H<sub>2</sub> during the PEC and EC process are summarized in Table S2 in Supporting information. As shown in Fig. 2d and Table S2 in Supporting information, the theoretical value and the measured value during the PEC process is much higher than that of the EC process. The H<sub>2</sub> evolution rate by PEC process is 34.44 μmol h<sup>-1</sup> cm<sup>-2</sup>, which is 3 times more efficient than the EC process (11.37 μmol h<sup>-1</sup> cm<sup>-2</sup>). However, some of the generated electrons on the cathode can be consumed by the reduction of the small intermediates formed by the degradation of MO, consequently, an obvious difference between the theoretical H<sub>2</sub> evolution rate and measured H<sub>2</sub> evolution rate during the PEC process is observed. The calculated Faradaic efficiency of H<sub>2</sub> during the PEC process (62%) is thus lower than that of EC process (96%).

Besides, the stability of the H<sub>2</sub> generation is confirmed by the curves of photocurrent density vs. time, which is steady and shows ignorable changes in 6 h H<sub>2</sub> experiment with BiVO<sub>4</sub> as the anode material during the PEC and EC processes (Fig. S3 in Supporting information). The stability is further confirmed by performing the MO degradation for five runs by PEC route. These experiments are carried out by applying the recycled BiVO<sub>4</sub> film to fresh MO solutions with the same concentration, and the results are shown in Fig. S4 in Supporting information. Since there is no obvious decrease in activity is observed after five runs, indicating that the BiVO<sub>4</sub> film owns outstanding stability and recyclability during the PEC reaction and it would be a promising candidate for the wastewater treatment and H<sub>2</sub> production. Additionally, the nanostructured BiVO<sub>4</sub> photocatalyst shows more excellent recycle performance than previous reports [33,38].

To investigate the origin of the enhanced PEC activity, the electrochemical property of BiVO<sub>4</sub> is performed by the electrochemical impedance spectroscopy (EIS). The EIS measurements are conducted at the same electrolyte solution. (Fig. S5a in Supporting information) shows the EIS Nyquist plots of BiVO<sub>4</sub> film in the dark and under the light illumination. Here, the EIS results are obtained by using a three-electrode cell system, thus the arc radius in Nyquist plot represents the charge transfer resistance on the working electrode interface. The diameter of the arc radius on the Nyquist plot in the presence of solar light (PEC process) is smaller than that in the absence of solar light (EC process), indicating the efficient charge separation and transport. Hence, the nanostructured BiVO<sub>4</sub> electrode film exhibited outstanding catalytic performance of degradation of azo dye and H<sub>2</sub> generation during the PEC process than that of EC process. Besides, the Bode phase plot of nanostructured BiVO<sub>4</sub> is shown in Fig. S5b. The result indicates that there is no current passing through the external circuit. And the nanostructured BiVO<sub>4</sub> shows the highest Bode phase at 0.25 Hz.

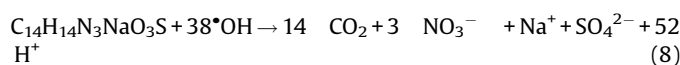
In order to detect the micromorphology, structure and surface of the catalysis after PEC degradation process, SEM image, XRD pattern and XPS analysis of the photoanode were conducted after PEC degradation process. As shown in Fig. S6a and b in Supporting information, the micromorphology and structure keep unchanged after PEC degradation process. Besides, after comparing the surface elements of the photocatalyst before and after catalytic action with XPS measurement (Fig. S6c), hardly any new elements could be detected or any element disappeared. The above results indicate that the physicochemical property of the nanostructured BiVO<sub>4</sub> could not be destroyed during the PEC degradation process.

This PEC system involving a photocatalytic oxidation process on the anode and a reduction process on the cathode is shown in Scheme 2. The half reactions on the photoanode side are described as follows: with the xenon light irradiation, the electrons of BiVO<sub>4</sub> film are excited from the valence band (VB) to the conduction band (CB), which producing positive holes (h<sup>+</sup>) in the VB and negative electrons (e<sup>-</sup>) in the CB (Eq. (5)). To avoid the recombination of photogenerated h<sup>+</sup> and e<sup>-</sup> and provide enough energy potential for



**Scheme 2.** Schematic illustration of MO degradation with simultaneous H<sub>2</sub> generation via PEC route.

H<sub>2</sub> generation, an external bias is introduced. Then the photo-generated e<sup>-</sup> travels through the interface of BiVO<sub>4</sub> electrode to the cathode by external circuit, while h<sup>+</sup> is involved in the oxidation reaction of the MO (Eq. (8)), via \*OH radicals formed through the reaction with OH<sup>-</sup> and H<sub>2</sub>O in the solution (Eqs. (6) and (7)). For the MO degradation, the \*OH radicals attack the azo band in the MO molecule and break down the N-N bond, and then the intermediates are degraded to small molecules and finally oxidized to CO<sub>2</sub> and H<sub>2</sub>O [39]. On the cathode of the PEC system, H<sub>2</sub>O as terminal electron acceptors is reduced to H<sub>2</sub> and OH<sup>-</sup> by accepting the electrons from cathode with assistance of Pt wire (Eq. (9)). OH<sup>-</sup> is then generated on the cathode for the continuously consuming on the photoanode side, forming the PEC process circle.



In summary, we prepared a nanostructured BiVO<sub>4</sub> film electrode for the degradation of azo dye and simultaneously H<sub>2</sub> production by PEC process. The BiVO<sub>4</sub> electrode presented a strong absorption from the UV to visible light range. The PEC process shows excellent catalytic activity of MO degradation and also H<sub>2</sub> production, which are both much higher than EC or PC process alone. We show that the wastewater treatment can be well integrated into the PEC water splitting, which may make the PEC water splitting economically feasible. The proposed PEC system shows the potential to be a sustainable and energy-saving way for simultaneous wastewater treatment and energy recovery.

### Acknowledgements

The authors gratefully acknowledge the financial support from National Natural Science Foundation of China (Nos. 21507011, 21677037, 21607027), China Postdoctoral Science Foundation (No. KLH1829017), and Ministry of Science and Technology of China (Nos. 2016YFE0112200, 2016YFC0203700).

References

- [1] S. Hameed, R.D. Cess, J.S. Hogan, *J. Geophys. Res. Oceans* 85 (1980) 7537–7545.
- [2] J.J. Griffin, E.D. Goldberg, *Geochimica. ET. Cosmochimica. Acta* 45 (1981) 763–769.
- [3] H. Hevy, W.J. Moxim, *Tellus. B* 41 (1989) 256–271.
- [4] S.S. Penner, *Energy* 16 (1991) 1417–1419.
- [5] J.Y. Jiang, M. Chang, P. Pan, *Environ. Sci. Technol.* 42 (2008) 3059–3063.
- [6] C.A. Reddy, M.P. Bryant, M.J. Wolin, *J. Bacteriol.* 110 (1972) 126–132.
- [7] X. Zong, H.J. Yan, G.P. Wu, et al., *J. Am. Chem. Soc.* 130 (2008) 7176–7177.
- [8] B. Cao, G.S. Li, H.X. Li, *Appl. Catal. B: Environ.* 194 (2016) 42–49.
- [9] Z.W. Chen, X.Y. Jiang, C.B. Zhu, C.K. Shi, *Appl. Catal. B: Environ.* 199 (2016) 241–251.
- [10] E. Gianotti, M. Taillades-Jacquin, Á. Reyes-Carmona, et al., *Appl. Catal. B: Environ.* 185 (2016) 233–241.
- [11] D.S. Hu, Y. Xie, L.J. Liu, et al., *Appl. Catal. B: Environ.* 188 (2016) 207–216.
- [12] B.H. Wu, D.Y. Liu, S. Mubeen, et al., *J. Am. Chem. Soc.* 138 (2016) 1114–1117.
- [13] H.H. Liu, D.L. Chen, Z.Q. Wang, H.J. Jing, R. Zhang, *Appl. Catal. B: Environ.* 203 (2017) 300–313.
- [14] Y.F. Zhao, B. Zhao, J. Liu, et al., *Angew. Chem. Int. Ed.* 55 (2016) 4215–4219.
- [15] Y.F. Zhao, X.D. Jia, G.I.N. Waterhouse, et al., *Adv. Energy Mater.* 6 (2016) 1501974.
- [16] L. Shang, B. Tong, H.J. Yu, et al., *Adv. Energy Mater.* 6 (2016) 1501241.
- [17] J.M. Liu, L. Han, H.Y. Ma, et al., *Sci. Bull.* 61 (2016) 1543–1550.
- [18] L.W. Zhang, C.Y. Lin, V.K. Valev, et al., *Small* 10 (2014) 3970–3978.
- [19] S.M. Sun, W.Z. Wang, D.Z. Li, L. Zhang, D. Jiang, *ACS Catal.* 4 (2014) 3498–3503.
- [20] J. Seo, T. Takata, M. Nakabayashi, et al., *J. Am. Chem. Soc.* 137 (2015) 12780–12783.
- [21] T. Reier, Z. Pawolek, S. Cherevko, et al., *J. Am. Chem. Soc.* 137 (2015) 13031–13040.
- [22] F. Jiang, Gunawan T. Harada, et al., *J. Am. Chem. Soc.* 137 (2015) 13691–13697.
- [23] L.L. Feng, G.T. Yu, Y.Y. Wu, et al., *J. Am. Chem. Soc.* 137 (2015) 14023–14026.
- [24] C.A. Downes, S.C. Marinescu, *J. Am. Chem. Soc.* 137 (2015) 13740–13743.
- [25] P.A. Williams, C.P. Ireland, P.J. King, et al., *J. Mater. Chem.* 22 (2012) 20203–20209.
- [26] L. Wang, M.H. Cao, Z.H. Ai, L.Z. Zhang, *Environ. Sci. Technol.* 48 (2014) 3354–3362.
- [27] K.X. Li, Z.X. Zeng, L.S. Yan, et al., *Appl. Catal. B: Environ.* 187 (2016) 269–280.
- [28] J. Ke, J. Liu, H.Q. Sun, et al., *Appl. Catal. B: Environ.* 200 (2017) 47–55.
- [29] M. Panizza, P.A. Michaud, G. Cerisola, C. Cominellis, *Electrochem. Commun.* 3 (2001) 336–339.
- [30] H. Tong, S.X. Ouyang, Y.P. Bi, et al., *Adv. Mater.* 24 (2012) 229–251.
- [31] K.J. McDonald, K.S. Choi, *Energy Environ. Sci.* 5 (2012) 8553–8557.
- [32] M. Zhou, J. Bao, Y. Xu, et al., *ACS Nano* 8 (2014) 7088–7098.
- [33] J.L. Zhang, Y. Lu, L. Ge, et al., *Appl. Catal. B: Environ.* 204 (2017) 385–393.
- [34] J. Bai, R. Wang, Y.P. Li, et al., *J. Hazard. Mater.* 311 (2016) 51–62.
- [35] S.K. Pilli, T.E. Furtak, L.D. Brown, et al., *Energy Environ. Sci.* 4 (2011) 5028–5034.
- [36] J.Q. Li, J. Zhou, H.J. Hao, L.W. Jie, *Appl. Surf. Sci.* 399 (2017) 1–9.
- [37] N. Myung, W. Lee, C. Lee, S. Jeong, K. Rajeshwar, *ChemPhysChem* 15 (2014) 2052–2057.
- [38] E. Aguilera-Ruiz, U. M.Garcia-Perez, M. Garza-Galvan, et al., *Appl. Surf. Sci.* 328 (2015) 361–367.
- [39] S.B. Xu, Y.F. Zhu, L. Jiang, Y. Dan, *Water Air Soil Pollut.* 213 (2010) 151–159.